

UNCLASSIFIED

AD NUMBER
AD914384
NEW LIMITATION CHANGE
TO Approved for public release, distribution unlimited
FROM Distribution authorized to U.S. Gov't. agencies only; Test and Evaluation; 29 AUG 1973. Other requests shall be referred to Naval Ordnance Lab., White Oak, MD 20910.
AUTHORITY
NOL ltr, 29 Aug 1974

THIS PAGE IS UNCLASSIFIED

NOLTR 73-117

NOL

**TECHNICAL
REPORT**

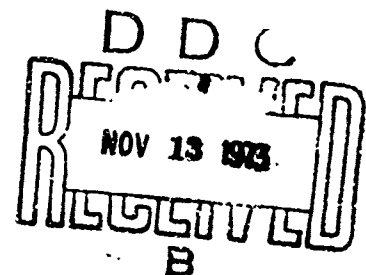
AD 914384

**THE SHOCK-TO-DETONATION TRANSITION IN TRIETHYLENE GLYCOL DINITRATE
(NOSET-A)**

**BY
J.W. Forbes
N.L. Coleburn**

**NAVAL ORDNANCE LABORATORY
WHITE OAK, SILVER SPRING, MD. 20910**

Distribution limited to U.S. Government Agencies
only; test and evaluation; 29 August 1973. Other
● requests for this publication must be referred to
NOL, Code 242.



**NAVAL ORDNANCE LABORATORY
WHITE OAK, SILVER SPRING, MARYLAND 20910**

THE SHOCK-TO-DETONATION TRANSITION IN TRIETHYLENE GLYCOL
DINITRATE (NOSET-A)

Prepared by:
J. W. Forbes
N. L. Coleburn

ABSTRACT: The detonation and detonation buildup properties of triethylene glycol dinitrate (NOSET-A) were evaluated in small-scale detonation and wedge tests. The detonation velocity is strongly affected by the temperature. Detonation propagates at 5950 m/sec when the heavily confined liquid at 60°F is initiated by a plane-wave booster. Failure however occurs when the NOSET-A is at 29°F. The detonation pressure at ~55°F is 170 kbars. NOSET-A transforms to detonation in the wedge test at transmitted pressures in the range of 110 - 130 kbars with a behavior similar to nitromethane.

EXPLOSION DYNAMICS DIVISION
EXPLOSIONS RESEARCH DEPARTMENT
NAVAL ORDNANCE LABORATORY
WHITE OAK, SILVER SPRING, MARYLAND

NOLTR 73-117

NOLTR 73-117

18 September 1973


The Shock-To-Detonation Transition in Triethylene Glycol
Dinitrate (NOSET-A)

This report gives results of laboratory detonation and shock impact tests which were performed in support of the NOSET-A Qualification Program.

This work was done under: ORD TASK-054-000/U2306.

The authors are grateful to D. Gillmore and N. Snowden of the Naval Ordnance Laboratory who assisted in the experiments.

ROBERT WILLIAMSON II
Captain, USN
Commander


C. J. ARONSON
By direction

CONTENTS

	Page
I. INTRODUCTION	1
II. EXPERIMENTAL	2
III. CONCLUSIONS	6
IV. REFERENCES	7

Tables

Table	Title	Page
1	Shock co-Detonation Measurements	8

ILLUSTRATIONS

Figure	Title	Page
1	Liquid Wedge-Test Arrangement	9
2	(A) The Effect of a Cylindrical Detonation of NOSET-A on a Steel Witness Plate at 60°F	10
	(B) Detonation Failure Occurs at 29°F	10
3	Smear Camera Record of Shock-to-Detonation Transition in a NOSET-A Wedge	11
4	x-t Diagram of Shock Transition in NOSET-A	12
5	Pressure (P) - Particle Velocity (u_p) of NOSET-A and Otto Fuel	13
6	Hugoniot Equation-of-State of NOSET-A and TNT	14

I. INTRODUCTION

This report describes tests to assess the initiation behavior and detonation properties of the liquid propellant, NOSET-A. NOSET-A is a clear, yellow liquid consisting of triethylene glycol dinitrate with 3% of dibutyl sebacate and 1% ethyl centralite, added respectively as a desensitizer and a stabilizer. The density of the liquid is 1.30 g/cm^3 at a temperature of 20°C . The explosive properties of NOSET-A to our knowledge have not been reported.

One purpose of this study was to obtain critical pressure* values for assessing the hazards of explosion in the event the propellant were exposed to a shock or blast environment. It is considered that the probability of any explosive material being detonated by mechanical shocks is a function of the shock pressure transmitted into the material. If the material is detonable and is subjected to a shock below its detonation pressure, chemical reaction will still occur and accelerate if the shock is of sufficient amplitude and duration. The shock will travel a measurable distance (called the run distance) within the explosive before detonation results. The lower the transmitted shock pressure the greater will be the run distance and the time before detonation occurs. Below some critical pressure however, detonation will not occur and reaction ordinarily will be quenched.

There are a number of tests which can give information on the critical pressure for detonation to result, e.g., calibrated gap tests. However the wedge test, reference 1 and Figure 1, is admirably suited to this measurement, and yields not only the critical pressure but the time and run distance within the explosive before a steady detonation wave is observed. In the test, a shock of known amplitude is transmitted to a wedge of the test explosive by a calibrated plane pressure pulse from an inert shocked material. The time and run distance are detected by measuring the velocity and position of the transmitted shock wave by high-speed smear camera photography. These measurements allow comparisons to be made of the sensitivity behavior of explosives when shock-initiated. The test can also compare explosives by determining the pressure and time required to induce significant reaction in them when they are shocked.

*The pressure needed to detonate an explosive at the 50% probability level.

Prior to the wedge experiments, it was necessary to determine whether the NOSET-A was detonable and if so, to determine its detonation properties. As will be shown in the next section of this report, the detonation and transition to detonation properties of NOSET-A are comparable to those of the explosive nitromethane² and are different from those of Otto Fuel II³. Otto Fuel II which is to be replaced by NOSET-A does not build to detonation in the NOL wedge test.

II. EXPERIMENTAL

A. DETONATION VELOCITY MEASUREMENTS. Some propellant materials subjected to strong mechanical shocks may be readily ignitable, however, they might undergo the transition to full detonation only with difficulty, i.e., under conditions of large size and heavy confinement. Before conducting more sophisticated experiments it was necessary to establish whether NOSET-A was detonable in the arrangements normally used for measuring initiation and detonation properties. Small-scale firings, at 29°F, 50°F, and 60°F with the liquid contained in metal cylinders, were used to assess the detonability of NOSET-A. High-speed smear camera photography was used to measure the shock wave velocity in the liquid. In these firings the propellant was confined in 8-inch long copper tubes having a 2-inch I.D. and 0.21-inch thick walls. One end of the tube was sealed with a 2-inch thick steel witness plate. Evenly spaced 0.5-inch diameter holes were drilled along a line and through the walls of the tubes. The holes were covered by a thin strip of plastic which was attached to the inner tube wall. The holes served as ports for viewing luminosity through the slit of the smear camera. Initiation of the NOSET-A was accomplished by a booster consisting of a 2-inch long by 2-inch diameter pentolite pellet and a pentolite-baratol plane wave generator.

The velocity measurements showed that the start and propagation of an energetic reaction in NOSET-A was strongly affected by the temperature. At 50°F and 60°F NOSET-A detonated. This was evident from the propagation velocity of 5950 m/sec and the 0.5-inch deep crater produced in the steel witness plate. The plate also showed considerable spall. The effect of the detonation at 60°F on the steel plate is shown in Figure 2a. At 29°F, however NOSET-A failed to detonate. Although ignition occurred under the conditions of confinement and boosting described above, detonation did not propagate. This fact was evident from both the high-speed smear camera photographs and the undented steel witness plate (see Figure 2b). In comparison, Otto Fuel II in the above geometry at 60°F shows signs of failure after 6-inches of propagation, yielding an overdriven non-steady shock velocity of 4950 m/sec. Thus in 2-inch diameter copper tubes, Otto Fuel II appears to be in a subcritical state since its detonation velocity³ in 1/2-inch diameter brass tubes is ~6000 m/sec.

B. DETONATION PRESSURE MEASUREMENTS. Air shock measurements at the end of detonating cylinders of NOSET-A were used to determine values of the detonation pressure and the isentropic exponent for the expansion of NOSET-A explosion products. In these measurements the setup was identical to the arrangement for measuring detonation velocities except that the 2-inch thick steel witness plate was removed from

one end of the copper cylinder. The NOSET-A was boosted as described above and the shock from the explosion emerging at the open end of the cylinder into air, was back-lighted using an exploding wire and a collimating lens⁴. The initial velocity of the air shock was determined by extrapolating the slope of smear camera trace to the end of the NOSET-A cylinder.

The initial shock velocity measured from NOSET-A detonating in air was 5800 m/sec. This velocity was used with the shock impedance equations derived in reference⁵ and the shock Hugoniot relations for air⁷ to obtain the detonation pressure and isentropic exponent of expansion for the explosion products. In these determinations, using the detonation velocity, D , of 5950 m/sec, measured in the above tests, we obtained a detonation pressure of 170 kbars and an isentropic exponent, γ , of 1.71. Using this value of γ we calculated the heat of detonation, Q , as 573 cal/g for NOSET-A, according to the relationship,

$$Q = \frac{D^2}{2(\gamma - 1)} \quad (1)$$

These values of the detonation pressure and heat of detonation are ~40% and ~80% greater respectively than similar values for Otto Fuel.

C. WEDGE TESTS. The experimental arrangement for the wedge tests is shown in Figure 1. The shock pressure imparted to the liquid propellant was varied by using calibrated explosive plane wave shock systems (Table 1). These systems were calibrated from free-surface velocity and shock velocity measurements of the driver plate material. The known Hugoniot equation-of-state of the driver plate material was then used to obtain the incident shock pressures produced by the systems. The transmitted pressure in NOSET-A was obtained by impedance matching.

In the test arrangement the liquid was contained within an indented wedge section of a Plexiglas plate. The inclined surface of the indented wedge section was machined at an appropriate angle (30° or 11°) to allow the formation of a liquid wedge of the desired maximum thickness. The Plexiglas plate was attached to the driver plate so that one surface of the propellant within the indented wedge section was in contact with the driver plate and the other propellant surface was in contact with the indented plexiglas wedge surface. An aluminized mylar strip was attached to the surface of the indented section to provide a reflective surface for detecting the emergence of the shock wave at the liquid-Plexiglas interface, using the reflected-light smear camera technique described previously.

1. Wedge Test Smear Camera Record. A smear camera record of a wedge experiment (Shock System 4 in Table 1) is shown in Figure 3 with time increasing from left to right. The sharp decrease in reflected light when shock waves are incident on reflecting surfaces allows the

camera to record the shock arrivals. These events appear as sharp light intensity changes on the camera record. The light intensity changes, designated (1) in the record, give information on the arrival of a shock wave at the surface of the shock driver plate. The change at (2) denotes the shock wave arrival at the free surface of a metal pellet attached to the driver plate surface. The difference between the times of arrival for these events, (1) and (2) is the transit time of the incident shock in the pellet. The pellet's thickness divided by this time gives an average shock velocity which permits the incident shock pressure, P_A in Table 1 to be obtained from knowledge of the driver plate material's Hugoniot equation-of-state^{8,9}. The velocity of the transmitted shock wave in the liquid wedge was determined by the slope of the line trace labeled (3).

After an induction period of 0.3 microsec, a detonation wave (4) propagates in the previously shock-compressed liquid propellant, catching and interacting with the, initially inert, steady shock wave at (5). The detonation becomes overdriven at point (6) in the liquid. The transmitted shock in this small portion of the run distance accelerates to a velocity near 8600 m/sec which is ~40% higher than the normal detonation velocity of NOSET-A. This overshoot phenomena is typical of the behavior noted in other liquid explosives, i.e., nitromethane² and some composite propellants¹⁰ and pressed TNT¹¹. The overshoot then decays into a normal steady state detonation (7). The point (8) is the detonation wave arrival at the constant thickness portion of the NOSET-A within the Plexiglas container.

The pictorial x-t diagram* of Figure 4 shows the wave propagation in the liquid propellant for detonation. An initial transmitted shock wave causes no measurable chemical reaction and the NOSET-A behaves like an inert liquid in which the shock wave velocity is constant. After a period of time, detonation occurs in the pre-compressed propellant near the driver plate-liquid interface. This overdriven detonation wave travels faster than the initial transmitted shock. Also, since it is moving into liquid that has been compressed to a higher density than the initially unshocked liquid, it is traveling, at a velocity faster than the steady detonation value, i.e., by a surplus velocity equal to the particle velocity behind the initial transmitted shock wave. Thus the detonation wave catches the initial transmitted shock and overshoots its steady velocity value. The "overshoot" decays rapidly however, and the wave becomes steady.

2. Wedge Tests Results. Table 1 lists values of the instantaneous shock velocity, D_N , measured in the regime (7) of the trace in Figure 3 where a steady state is reached. These values are only slightly larger (within 10%) than the value of the detonation velocity of NOSET-A measured with the liquid confined in 2-inch diameter copper tubes. The initial shock velocity, i.e., the value at small wedge

*The events depicted in the diagram are not shown scaled to their actual occurrence.

thickness associated with region (3) of Figure 3, is designated U_N in Table 1. By impedance matching with this shock velocity for the first three systems in Table 1, and the pressure-particle velocity relation of the driver plate material, we obtained a pressure-volume (Hugoniot) curve for the propellant where no reaction was assumed. These data are P_N and V_N in Table 1. If reaction results from the shock impact the results will deviate from the unreacted curve. This deviation allows detection of the pressure regime where significant reaction occurs and will be discussed later.

The distance, X_N , in Table 1, is the distance from the driver plate-interface to a point in the liquid where the transition from an inert shock to a single steady detonation wave is complete. The data show that the distance, X_N decreases ~30% when the transmitted shock pressure P_N , is increased from 133 to 152 kbars. In one case, however, when the transmitted shock was delivered by System No. 7 in Table 1, initiation occurred immediately at the driver plate-liquid interface. The instantaneous shock velocity was constant throughout the shock run and had a value of 7370 m/sec. This value is ~20% greater than the normal NOSET-A detonation velocity and indicates that the incident shock impact initiated overdriven detonation.

It is apparent from the data in Table 1 that NOSET-A will transform to detonation under the shock impacts in the wedge test at a critical pressure between 114 - 130 kbars. This result indicates that NOSET-A is more shock sensitive than Otto Fuel II which did not display detonation build-up in the wedge test geometry used here. It is possible however that Otto Fuel II would behave differently in a larger wedge size. The detonation velocity data indicates it has a larger failure diameter than NOSET-A. On the other hand the build-up characteristics of NOSET-A are similar to the transition of nitromethane as first described in reference 2. Nitromethane however is somewhat more shock-sensitive; its critical pressure for a shock transition is between 80 - 90 kbars.

In Figure 5 the pressure-particle velocity curves for NOSET-A and Otto Fuel II³ are given. A comparison between the two curves shows that the two propellants are quite similar in their dynamic compressibility characteristics. (The pressure and particle velocity are related to the compression by the conservation of mass and momentum.) The data however represent unreacted shock states. When chemical reaction occurs the energy evolved causes the transmitted shock to accelerate. This behavior is indicated in Figure 5 by a large offset in the $P-u_p$ data. It is probable that the data above ~130 kbar in Figure 5 is affected by chemical reaction. Consequently, that data was not used to determine the unreacted shock states in the $P - V$ plane.

The dynamic compressibility (Hugoniot) curve obtained from the unreacted $P-u_p$ data is plotted in Figure 6 and compared there with a similar curve for TNT. As expected, the NOSET-A curve lies to the right of the curve for TNT, i.e., NOSET-A is substantially more compressible than TNT.

III. CONCLUSIONS

In summary, the wedge test results indicate that NOSET-A can be detonated by shock pressures in the range of 110 - 130 kbars.

In comparison with Otto Fuel II, NOSET-A has a smaller detonation failure diameter. Our experience with Otto Fuel II indicates that it is less shock sensitive than NOSET-A.

The detonability (critical diameter) of NOSET-A is strongly affected by the temperature. Detonation propagates at 5950 m/sec when heavily-confined NOSET-A is initiated at 60°F by plane wave boosting. Detonation failure occurs when NOSET-A is at 29°F.

The detonation pressure of NOSET-A initially at 60°F, is 170 kbars, which is ~30% greater than the detonation pressure of Otto Fuel II.

IV REFERENCES

1. S. J. Jacobs, T. P. Liddiard, Jr. and B. E. Drimmer, Ninth International Symposium on Combustion, Academic Press Inc., New York, N. Y. (1963)
2. A. W. Campbell, W. C. Davis, and J. R. Travis, Phys of Fluids 4, 498 (1961), *ibid* 4, 511 (1961)
3. H. D. Jones, L. A. Roslund, " L. Coleburn, J. N. Ayres, "The Detonation Properties and Unreacted Shock States of Otto Fuel," (T1)(U) NOLTR 69-111, (17 Jul 1969), (C)
4. T. P. Liddiard, Jr. and B. E. Drimmer, J. Soc. Motion Picture Television Engrs. 70, 106 (1961)
5. N. L. Coleburn, "Chapman-Jouguet Pressures of Several Pure and Mixed Explosives," NOLTR 64-58, (25 Jun 1964)
6. J. Hilsenrath and M. Klein, "Table of Thermodynamic Properties of Air in Chemical Equilibrium Including Second Virial Corrections from 1500°K to 15,000°K"
7. AEDC-TDR-63-16 (Aug 1963) also J. Hilsenrath and M. Klein, "Tables of Thermal Properties of Air," NBS circ. 564, Wash., D.C. (1953)
8. M. H. Rice, R. G. McQueen and J. M. Walsh, "Compression of Solids by Strong Shock Waves," Solid State Physics, Vol. 6 edited by F. Seitz and D. Turnbull, Academic Press, Inc., New York (1958)
9. N. L. Coleburn, "The Dynamic Compressibility of Solids from single experiments using Light-Reflection Techniques," NAVWEPS Rpt 6026 (31 Oct 1960)
10. N. L. Coleburn, "Sensitivity of Composite and Double Base Propellants to Shock Wave," AIAA Jour. 4, 521 (1968)

Table 1

SHOCK-TO-DETONATION MEASUREMENTS

Shock System Explosive Thickness No.	Shock Driver Plate Thickness (cm)	Shock Velocity U_N (mm/ μ sec)	Stress P_A (Kbar)	Detonation Velocity D_N (mm/ μ sec)	Distance X_N (mm)	Stress P_N (Kbar)	Particle Velocity u_p (mm/ μ sec)	Relative Volume V_N/V_0
1	2.54 AP	1.27 Brass	209	3.54	-	43.0	0.94	.734
2	2.54 AP	1.27 Aluminum	188	4.28	-	84.0	1.50	.650
3	2.54 TNT	1.27 Aluminum	246	4.76	-	114	1.84	.613
4	2.54 Comp B	1.27 Aluminum	264	5.43	4.5	133	1.90	-
5	2.54 Comp B	1.27 Aluminum	307	5.00	3.5	142	2.19	-
6	2.54 Comp B	1.27 Aluminum	298	5.65	2.7	152	2.08	-
7	2.54 Comp B	0.74 Plexiglas	187	-	0.0	209	2.19	-

NOLTR 73-117

A - Attenuator

N - NOSET-A

*These values are obtained by impedance matching for the initial transmitted shock where no reaction was assumed.

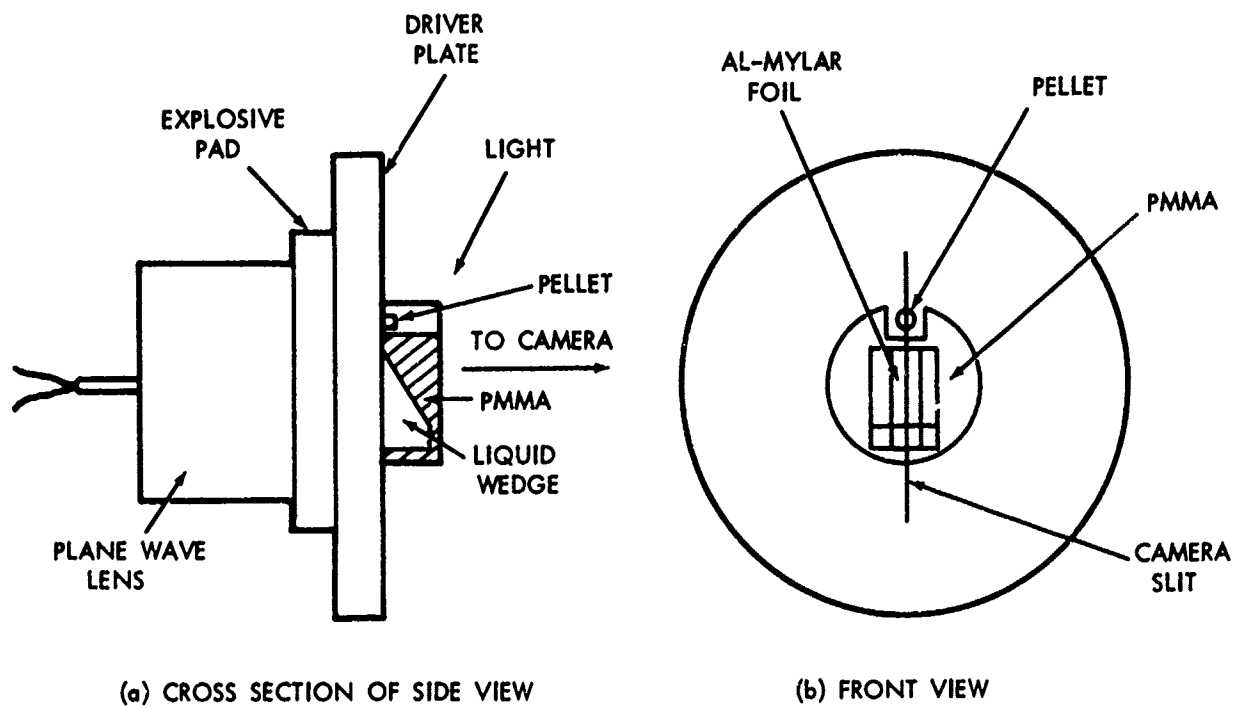


FIG. 1 (U) LIQUID WEDGE-TEST ARRANGEMENT (U)

UNCLASSIFIED
NOLTR 73-117



A. 60°F



B. 29°F

FIG. 2 (U) A. THE EFFECT OF A CYLINDRICAL DETONATION OF NOSET-A ON A
STEEL WITNESS PLATE AT 60°F
B. DETONATION FAILURE OCCURS AT 29°F

UNCLASSIFIED

UNCLASSIFIED
NOLTR 73-117

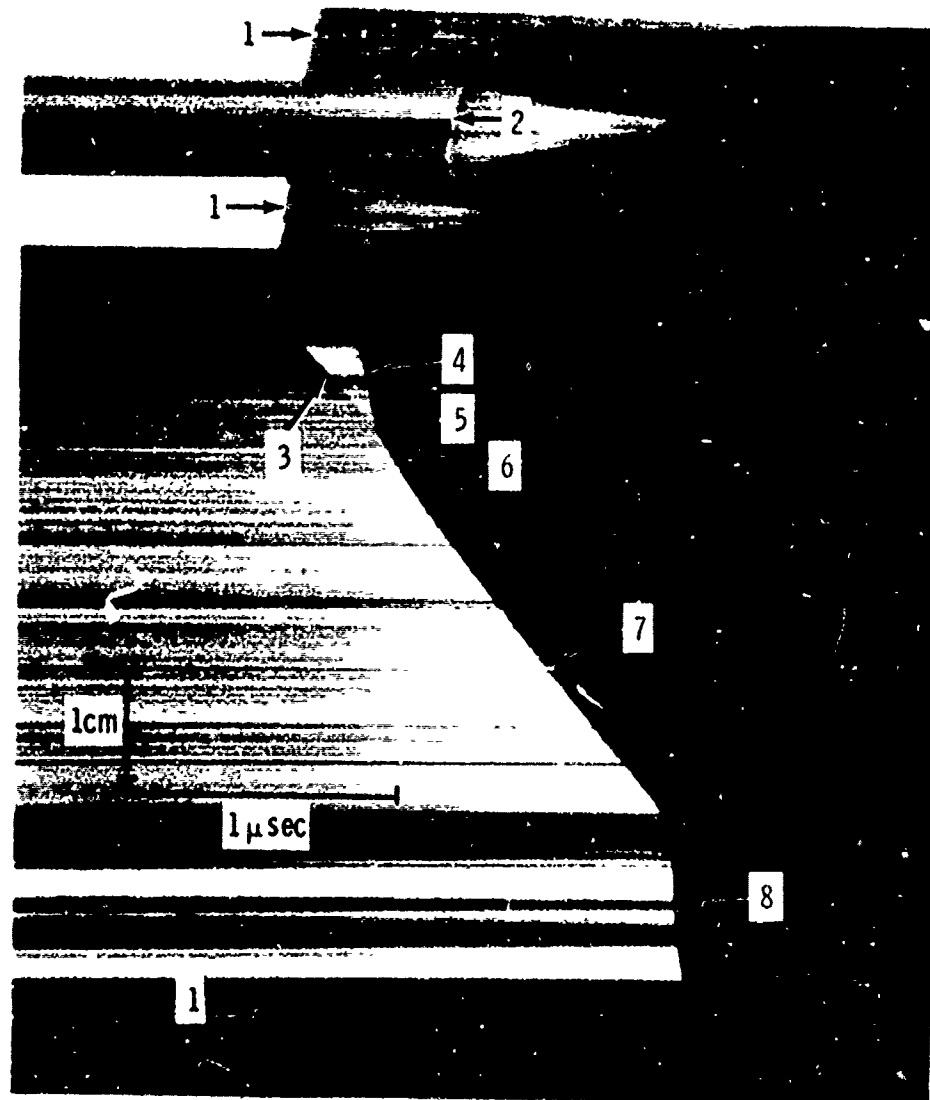


FIG. 3 (U) SMEAR CAMERA RECORD OF SHOCK-TO-DETONATION
TRANSITION IN A NOSET-A WEDGE (U)

UNCLASSIFIED

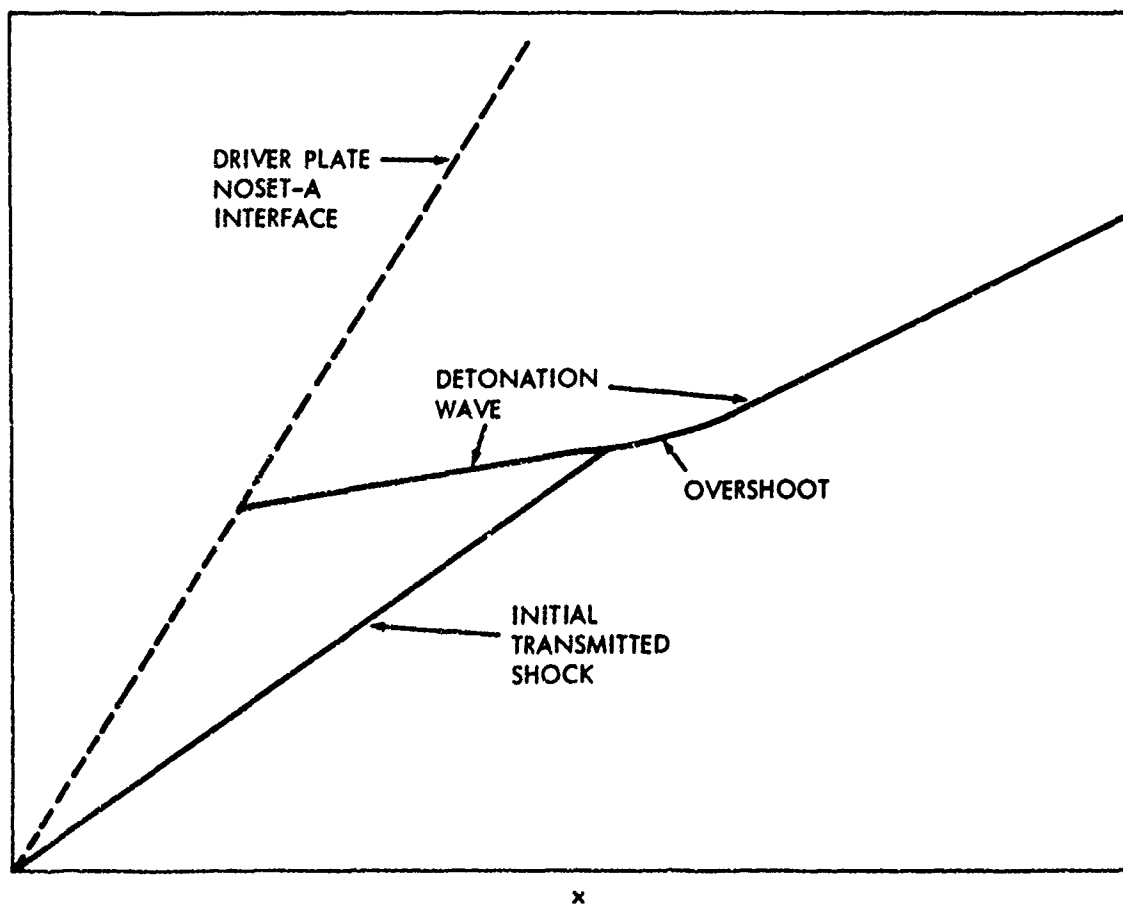


FIG. 4 (U) $x-t$ DIAGRAM OF SHOCK TRANSITION IN NOSET-A (U)

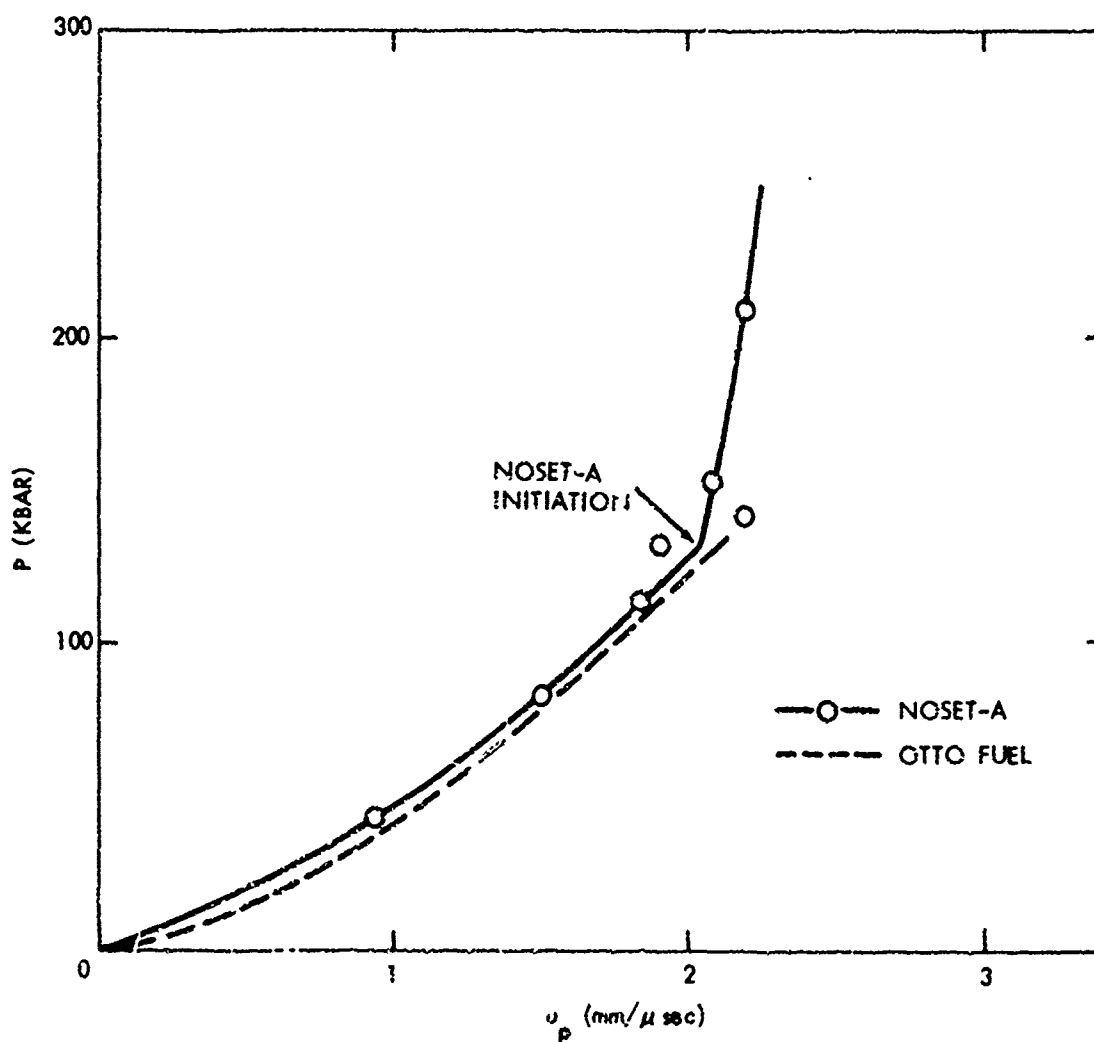


FIG. 5 (U) PRESSURE (P) - PARTICLE VELOCITY (u_p) OF NOSET-A AND OTTO FUEL (U)

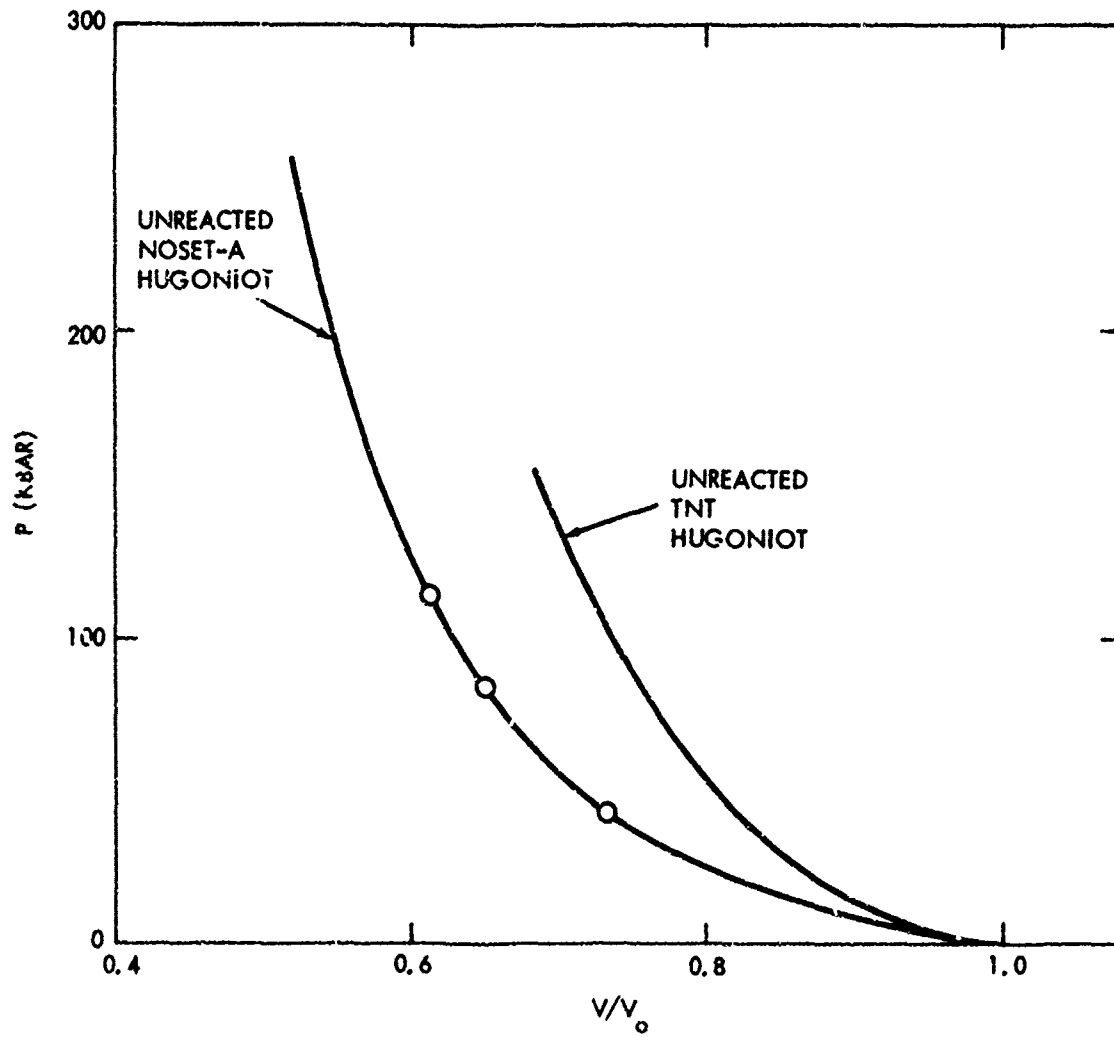


FIG. 6 (U) HUGONIOT EQUATION-OF-STATE OF NOSET-A AND TNT (U)

DISTRIBUTION

Copies

Commanding Officer
Naval Ordnance Station
Indian Head, Maryland 20640
M. Hoopnaak (5722C)
Technical Library

2

Commander Officer
Naval Underwater Systems Center
Newport, Rhode Island 02840
R. J. Heffernan (SB 331)
LAISI (Technical Library)

Gould, Inc.
Torpedo Mk 48 Program Office
18901 Euclid Avenue
Cleveland, Ohio 44117
E. Carmen

Commander, Naval Undersea Center
Pasadena Laboratory
3202 E. Foothill Boulevard
Pasadena, California 91107
Code 352

Commander
Naval Air Systems Command
Department of the Navy
Washington, D.C. 20371
AIR 50174 NAVAIR Library

Commander
Naval Facilities Engineering Command
Department of the Navy
Washington, D.C. 20360

DISTRIBUTION (Cont.)

Copies

Commander
Naval Ordnance Systems Command
Department of the Navy
Washington, D.C. 20360
ORD-10632 (NOSC Tech Library)
ORD-033
ORD-054
ORD-048
PMO-4021
ORD-035C2 (J. Nicolai)
ORD-0541 W. August

2

Commander
Naval Ship Systems Command
Department of the Navy
Washington, D.C. 20360

Commander
U.S. Marine Corps
Washington, D.C. 20380

Naval Academy
Annapolis, Maryland
Hd. Weapons Dept 21402

Commander
Naval Air Development Center
Johnsville, Pennsylvania 18974
Aviation Armanent Laboratory

Commander
U.S. Naval Air Test Center
Patuxent River, Maryland 20670

Commanding Officer
Naval Explosive Ordnance Disposal Facility
Indian Head, Maryland 20640
Library Division

Surperintendent
Naval Post Graduate School
Monterey, California 93940
Library (Code 2124)

Director
Naval Research Laboratory
Washington, D.C. 20390
Tech Information Section

2

DISTRIBUTION (Cont.)

Copies

Office of Naval Research
Department of the Navy
Arlington, Virginia 22217
Code 429
Technical Library

Commanding Officer and Director
U.S. Naval Ship Research and Development Laboratory
Panama City, Florida 32402

Commander
Naval Undersea Research and Development Laboratory
3202 F. Foothill Boulevard
Pasadena, California 91107

Commander
Naval Weapons Center
China Lake, California 93555
Code 556
Technical Library (Code 753)
Mallory (4544)
Code 454
Code 4541

Commanding Officer
Picatinny Arsenal
Dover, New Jersey 07801
Library
P. Harris

Commanding General
Redstone Arsenal
Huntsville, Alabama 35809
Technical Library

Commanding General
White Sands Proving Ground
White Sands, New Mexico 88002

Chief of Staff
U.S. Air Force
Washington, D.C. 20350
AFORD-AR

Commander
Air Force Cambridge Research Center
L. G. Hanscom Field
Bedford, Massachusetts 01730

NOLTR 73-117

DISTRIBUTION (Cont.)

Copies

AFWL (WLIL)
Kirtland AFB, New Mexico 87117

Army Materiel Command
Department of the Army
Washington, D.C. 20315
R&D Division

U.S. Army Research Office
Box CM
Duke Station
Durham, North Carolina 27706

Redstone Scientific Center
Chief, Documents
U.S. Army Missile Command
Redstone Arsenal, Alabama 35800

Commander
Frankford Arsenal
Philadelphia, Pennsylvania 19137
Mr. D. Askin

Commanding Officer
Harry Diamond Laboratories
Connecticut Avenue & Van Ness St., N.W.
Washington, D.C. 20438
ORD Development Lab
K. Warner

Missile and Space Systems Branch (OOYEG)
Hill AFB, Utah 84401

Commanding Officer
Air Force Missile Development Center
Holloman AFB, New Mexico 88330
Technical Data

Director
Applied Physics Laboratory
Johns Hopkins University
8621 Georgia Avenue
Silver Spring, Maryland 20910
Chemical Propulsion Information Agency
Dr. P. L. Nichols

DISTRIBUTION (Cont.)

Copies

Pittsburgh Mining & Safety Research Center
U.S. Bureau of Mines
Explosives Research Center
4800 Forges Avenue
Pittsburgh, Pennsylvania 15213
Richard Watson

Director
Defense Nuclear Agency
Washington, D.C. 20305

Defense Documentation Center
Cameron Station
Alexandria, Virginia 22314
TIPCR

2

National Aeronautics & Space Administration
Headquarters
600 Independence Avenue
Washington, D.C. 20546

Commanding Officer
Naval Weapons Evaluation Facility
Kirtland Air Force Base
Albuquerque, New Mexico 87117

Commander
U.S. Naval Weapons Laboratory
Dahlgren, Virginia 22448
Technical Library

Commanding Officer
Naval Weapons Station
Yorktown, Virginia 23491
Code 50

Commanding Officer
U.S. Naval Weapons Station
Concord, California 94520
Qual Eval Lab

Commander
Naval Missile Center
Point Mugu, California 93041

DISTRIBUTION (Cont.)

Copies

Director
Strategic Systems Projects Office
Department of the Navy
Washington, D.C. 20360

Commander
Naval Ship Research and Development Center
Norfolk Naval Shipyard
Norfolk, Virginia 23511
Underwater Explosions Research Division

U.S. Army Aberdeen Research and Development Center
Ballistics Research Laboratory
Aberdeen Proving Ground
Aberdeen, Maryland 21005
Technical Library

University of California
Los Alamos Scientific Laboratory (Director)
P. O. Box 1663
Los Alamos, New Mexico 87544
Library

Denver Research Institute
University of Denver
Denver, Colorado 80210

General Electric Company
Missile & Space Division
P. O. Box 8555
Philadelphia, Pennsylvania 19101
T. W. Kennedy

IIT Research Institute
Illinois Institute of Technology
10 West 35th Street
Chicago, Illinois 60616

University of California
Lawrence Livermore Laboratory
P. O. Box 808
Livermore, California 94550
Technical Information Division

Naval Ship Engineering Center
Center Building
Prince Georges Center
Hyattsville, Maryland 20782

NOLTR 73-117

DISTRIBUTION (Cont.)

Copies

Chief of Naval Material (DNL)
Washington, D.C. 20360

Naval Ship Research and Development Center
Bethesda, Maryland 20034
Technical Library
R. C. Allen, Code 012

Naval Underseas Center
San Diego, California 92132

R. Stresau Laboratory
Star Route
Spooner, Wisconsin 54081

UNCLASSIFIED

Security Classification

DOCUMENT CONTROL DATA - R & D		
<i>Security classification of title, body of abstract and indexing annotation must be entered when the overall report is classified</i>		
1. ORIGINATING ACTIVITY (Corporate author) Naval Ordnance Laboratory White Oak, Silver Spring, Maryland 20910		2a. REPORT SECURITY CLASSIFICATION UNCLASSIFIED
		2b. GROUP
3. REPORT TITLE THE SHOCK-TO-DETONATION TRANSITION IN TRIETHYLENE GLYCOL DINITRATE (NOSET-A)		
4. DESCRIPTIVE NOTES (Type of report and inclusive dates)		
5. AUTHOR(S): (First name, middle initial, last name) J. W. Forbes and N. L. Coleburn		
6. REPORT DATE 18 September 1973	7a. TOTAL NO. OF PAGES 14	7b. NO. OF REFS 10
8a. CONTRACT OR GRANT NO.	9a. ORIGINATOR'S REPORT NUMBER(S) NOLTR 73-117	
8b. PROJECT NO. ORD Task-054-000/U2306		
c.	9b. OTHER REPORT NO(S) (Any other numbers that may be assigned this report)	
d.		
10. DISTRIBUTION STATEMENT Distribution limited to U.S. Government Agencies only; test and evaluation; 29 August 1973. Other requests for this publication must be referred to NOL Code 24.		
11. SUPPLEMENTARY NOTES		12. SPONSORING MILITARY ACTIVITY Naval Ordnance Systems Command Washington, D.C. 20360
13. ABSTRACT The detonation and detonation buildup properties of triethylene glycol dinitrate (NOSET-A) were evaluated in small-scale detonation and wedge tests. The detonation velocity is strongly affected by the temperature. Detonation propagates at 5950 m/sec when the heavily confined liquid at 60°F is initiated by a plane-wave booster. Failure however occurs when the NOSET-A is at 29°F. The detonation pressure at 755°F is 170 kbars. NOSET-A transforms to detonation in the wedge test at transmitted pressures in the range of 110 - 130 kbars with a behavior similar to nitromethane.		

UNCLASSIFIED

Security Classification

14 KEY WORDS	LINK A		LINK B		LINK C	
	ROLE	WT	ROLE	WT	ROLE	WT
Propellant						
Detonation						
Shock						
Overshoot						
Sensitivity						
Triethylene						
Glycol						
Dinitrate						
NOSET-A						

UNCLASSIFIED

Security Classification